Secondary-ion-mass spectrometry and near-field studies of Ti:$LiNbO_3$ optical waveguides

F. Caccavale, P. Chakraborty,[a] and A. Quaranta
Università di Padova, Dipartimento di Fisica, via Marzolo 8, 35131 Padova, Italy

I. Mansour and G. Gianello
Università di Padova, Dipartimento di Elettronica ed Informatica, via Gradenigo 6/A, 35131 Padova, Italy

S. Bosso, R. Corsini, and G. Mussi
Pirelli Cavi Spa, Divisione Italia, viale Sarca 202, 20126 Milano, Italy

(Received 4 August 1994; accepted for publication 12 June 1995)

Secondary-ion-mass spectrometry (SIMS) and near-field (NF) methods have been applied to study Ti:$LiNbO_3$ optical waveguides. Ti concentration as a function of diffusion process parameters has been studied by the SIMS method. The main determining factors that were found to affect the depth-diffusion behavior of titanium in $LiNbO_3$ slab waveguides are the initial thickness of the dopant film and the diffusion temperature. Anisotropy in the diffusion rate for X- and Z-cut crystal directions has been observed. The propagating-mode NF method has been applied to the refractive index profile reconstruction for single-mode optical channel waveguides. A sharp change in the index at the air–guide interface has been observed, as expected. The dependence of refractive index change on Ti concentration has been found to be nonlinear, such as quadratic, approximately. © *1995 American Institute of Physics.*

I. INTRODUCTION

Lithium niobate ($LiNbO_3$) is one of the most popular dielectric materials for integrated optics.[1] It is characterized by low propagation loss (~0.1 dB/cm), ease in fabrication, and by utilizing its high electro-optic figure of merit it allows optical modulators and/or switches to be made for high-speed modulation, switching, and routing of optical signals.

The refractive index increase to realize an optical waveguide is usually achieved by locally doping the $LiNbO_3$ crystal with titanium at high temperature[2] or by ion exchange in which lithium ions of the substrate material are exchanged by hydrogen ions (protons) of the acid.[3,4] A large variety of integrated optical devices has been demonstrated where these two techniques have been employed.[5]

Although the procedure to fabricate high-quality Ti:$LiNbO_3$ optical devices has been known for more than 1 decade, it is important to make a systematic study of the diffusion behavior of titanium in $LiNbO_3$ for the optimization of the refractive index parameters in order to tailor the desired optical waveguides.

Secondary-ion-mass spectrometry (SIMS) is a powerful analytical tool to study the in-depth concentration profiles of the dopants because of its extremely high sensitivity and significant depth resolution.[6] The refractive index profile can be determined using one of the efficient optical measurements, such as effective index method (m line)[7,8] and near field (NF) method.[9,10] The knowledge of the interrelationship between the refractive index change and the dopant concentration provides a tool to reconstruct the refractive index profile. Some articles have dealt with the problem of the determination of refractive index changes in Ti-diffused $LiNbO_3$ optical waveguides.[11,12] For example, in one article a linear dependence between the extraordinary refractive index change and titanium concentration was obtained,[11] whereas in others a nonlinear relationship between refractive index change and titanium concentration was found.[12]

The present study reports Ti dopant concentration profiles in $LiNbO_3$ as function of process parameters, using SIMS analysis. It also presents a method to reconstruct the refractive index of Ti:$LiNbO_3$ waveguides using the refracted NF method, and how to relate the index change to Ti concentration. In Sec. II we report the results on the characterization of Ti diffusion process. In this step we have used slab waveguides, realized more simply in comparison to channel waveguides, permitting a complete analysis of the diffusion process. Later on, in Sec. III, we report results on optimization of refractive index profiles in channel waveguides by means of NF analysis, utilizing parameters derived in Sec. II. In Sec. IV the relation between Ti concentration and the corresponding index change is derived.

II. Ti:$LiNbO_3$ SLAB WAVEGUIDES

A. Experiment

Polished $LiNbO_3$ crystalline samples (Crystal Technology, Inc.) cut (X and Z directions) by Pirelli SpA, of $10\times10\times1\ mm^3$ dimension, were cleaned in successive baths of trichloroethylene, de-ionized water, and acetone using ultrasonic cleaner. Titanium films were deposited on $LiNbO_3$ substrates by an Alcatel rf magnetron sputtering machine, operating at a frequency of 13.56 MHz. The Ti target was water cooled. Sputtering was done in argon atmosphere at a pressure of 0.5 Pa. The power level was 150 W. Typically, the sputtering rate was 330 Å/min. Deposited film thicknesses were measured by a Dework V profilometer.

---
[a]Permanent address: Saha Institute of Nuclear Physics, 1/AF Bidhan Nagar, Calcutta 700064, India.

TABLE I. Process and diffusion parameters for Ti films diffused in $LiNbO_3$ (diffusion time: 8 h).

Sample no.	Ti thickness (Å)	Diffusion temp. (°C)	D ($\mu m^2/h$)	D_0 (10^8 $\mu m^2/h$)	Q (eV)
Z1	700	900	0.0770		
Z2	700	1000	0.6213		
Z3	700	950	0.2728	2.69	2.1777
Z4	500	950	0.3021		
Z5	500	1000	0.6726		
X1	700	900	0.1839		
X2	700	1000	0.3972		
X3	500	900	0.0820	0.333	2.0037
X4	500	1000	0.3805		
X5	500	950	0.1884		

Slab waveguides were prepared by the diffusion of the film material into the substrates by placing the samples into a tube furnace with three temperature zones provided with a digital temperature controller (±1 °C) under a flow of atmospheric air of 40 ℓ/h. The detailed procedure was described earlier.[6]

SIMS measurements of the diffused samples were performed using a CAMECA ims 4f ion microscope equipped with a normal incidence electron gun used to compensate the surface charge buildup while profiling insulating samples without any need to cover the surface with a metal film. Concentration profiles were obtained by 14.5 keV Cs^+ bombardment and by negative secondary-ion detection. The measured ion yield of each species at any instant lies within ±5% deviation. The erosion speed was evaluated by measuring the depth of the erosion crater at the end of each analysis by means of a profilometer Tencor Alpha Step. The maximum deviation in measuring a certain depth by this instrument is of the order of 5%. The calibration of the Ti profiles was made by means of the measurement of the total Ti dose in the as-deposited films using Rutherford backscattering spectrometry (RBS) analysis with 2.2 MeV $^4He^+$ beam ($\theta=160°$).

B. Results and discussions: SIMS analysis

The main parameters that affect and control the dopant concentration depth profiles are the initial thickness of the film and the diffusion temperature.[6] In order to obtain information regarding the anisotropy of the diffusion process, lithium niobate substrates with two different crystal cut directions were analyzed. Table I shows the experimental process parameters for two different (X and Z) crystal cut directions.

Figure 1 shows SIMS concentration profiles of titanium atoms in Z-cut slab waveguides at various diffusion temperatures for 500- and 700-Å-thick Ti films. Figure 2 shows the concentration depth profiles of titanium atoms for X cut for the same film thicknesses and diffusion condition. The Ti distribution in both cases is seen to be strongly affected by the temperature. The penetration depth is found to increase up to about 8 μm with a decrease in the maximum concentration at the surface of about 2–3 times with an increase of

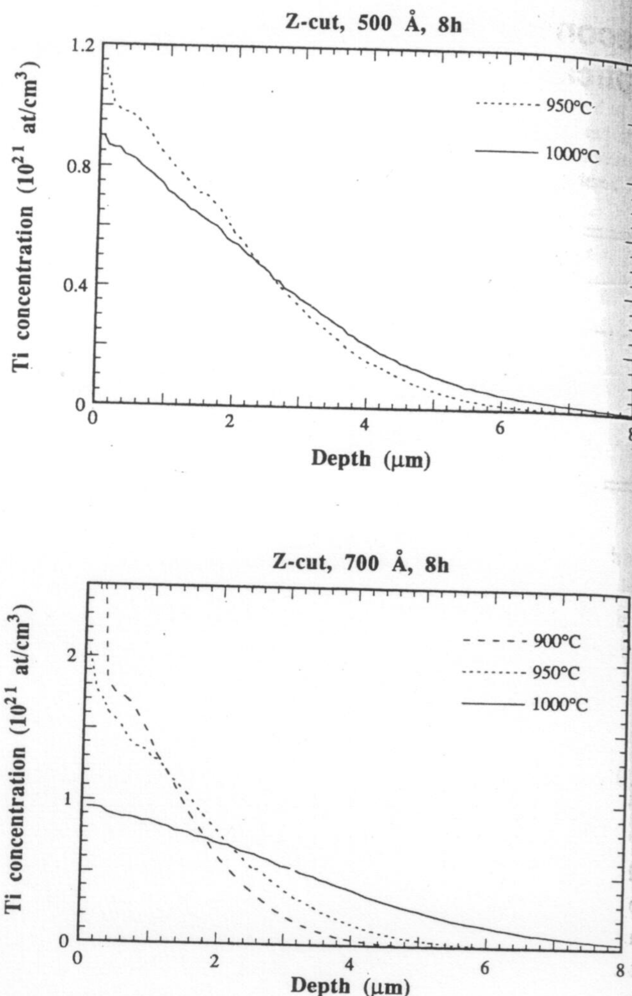

FIG. 1. SIMS depth profiles of Ti diffused in Z-cut $LiNbO_3$ slab waveguides.

temperature of 100 °C. In the case of 900 °C diffusion temperature the films are seen not to get completely diffused.

The measured profiles demonstrate that the one-dimensional (planar) diffusion process can be described by the standard Fick-type diffusion equation where the boundary is kept at a constant concentration C_0, provided the titanium reservoir is not exhausted during the diffusion,

$$\frac{\partial C(y,t)}{\partial t}=D\,\frac{\partial^2 C(y,t)}{\partial y^2},$$

$$C(0,t)=C_0,\quad y=0, \tag{1}$$

$$C(y,0)=0,\quad y>0,$$

where C is the titanium concentration, y is the direction normal to the substrate surface, and D is the diffusion coefficient. The solution is the complementary error function,[13]

$$C(y,t)=C_0\ \mathrm{erfc}\left(\frac{y}{2\sqrt{Dt}}\right)\quad (t\leq t_1). \tag{2}$$

y is the depth measured from the diffusion surface and t is the total diffusion time. The surface concentration C_0 can be regarded as the maximum solubility of Ti into $LiNbO_3$ at a

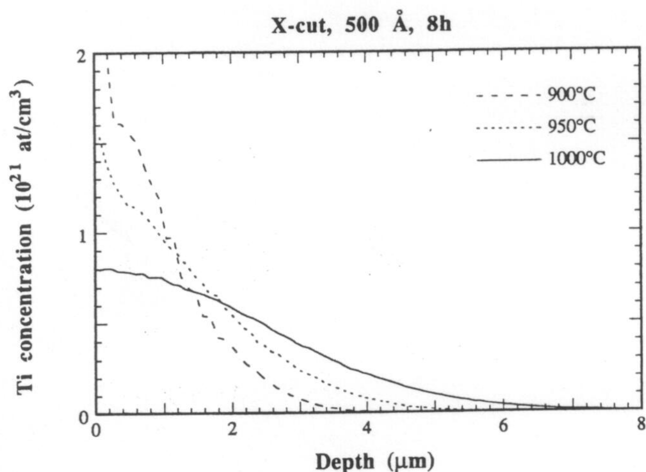

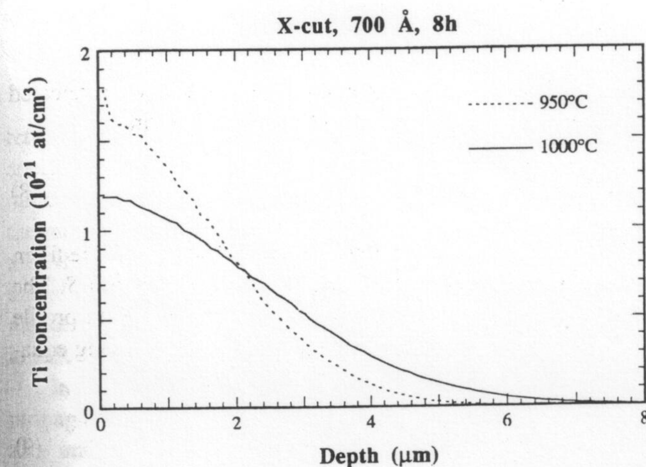

FIG. 2. SIMS depth profiles of Ti diffused in X-cut $LiNbO_3$ slab waveguides.

given temperature. At the time $t=t_1$, which can be evaluated from the law of mass conservation, the reservoir is depleted. With ρ being the mass density, M the molecular weight of the titanium, N_A Avogadro's number, and τ the initial film thickness, one can write

$$C_0\int_0^{+\infty} \operatorname{erfc}\left(\frac{y'}{2\sqrt{Dt}}\right) dy' = Ç\tau, \quad Ç=\frac{\rho N_A}{M}. \tag{3}$$

The integral can be solved analytically. Therefore, the time t_1 to guarantee complete in-diffusion can be expressed as

$$t_1=\left(\frac{Ç\tau}{2C_0}\right)^2 \frac{\pi}{D}.$$

For times much larger than t_1 the diffusion process enters in the annealing phase. The diffusion profile can be approximated by a Gaussian with a surface concentration c_0 below the solid solubility,

$$C(y,t)=c_0(t)\exp\left(\frac{-y^2}{4Dt}\right), \qquad c_0(t)=\frac{Ç\tau}{\sqrt{\pi Dt}}, \quad t\gg t_1. \tag{4}$$

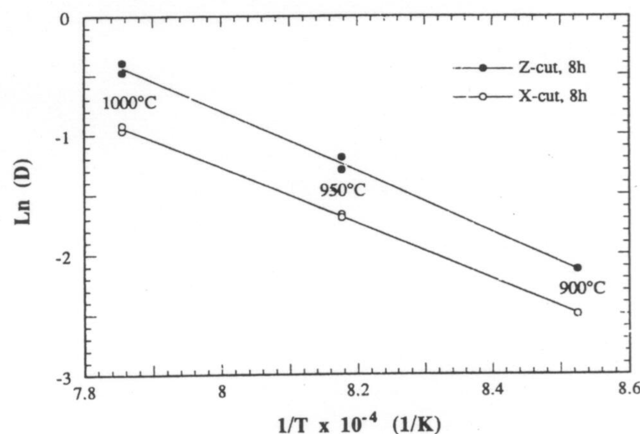

FIG. 3. Arrhenius plots of Z- and X-cut slab waveguides.

In the case of uncompletely diffused Ti films experimental SIMS profiles have been fitted by erfc functions (2) with C_0 and D parameters. When a complete film diffusion has been observed a Gaussian fit (4) is used.

Figure 3 presents the plot of diffusion coefficient as a function of $1/T$ for all analyzed samples. The diffusion coefficient D is related to the diffusion temperature by the well-known Arrhenius equation

$$D=D_0 \exp\left(\frac{-Q}{kT}\right),$$

where D_0 is the diffusion constant, Q is the activation energy, k is the Boltzmann constant, and T is the diffusion temperature. Knowing D at different temperatures one can calculate D_0 and Q (Table I). As seen in Fig. 3, the diffusion coefficient in the case of the Z-cut direction is approximately twice that in the case of the X-cut direction, showing an anisotropy of the diffusion process in the crystal.

The lithium depth profile, measured by SIMS, suffers a surface depletion in a 1-μm-thick layer. After this region Li profile reaches a steady-state value. The Li outdiffusion phenomenon, commonly encountered during Ti diffusion treatment, could be thought as the superposition of two effects:

(i) broad, steady-state depletion (depth≈87 μm), due to the fact that Li ions are small and mobile, and can be redistributed easily in the crystal structure, and
(ii) narrow depletion (depth≈1 μm), which is function of the crystal surface state and diffusion conditions.

In our case, the estimated whole index increment due to Li loss is negligible compared with that caused by Ti diffusion.[14]

It is known that the Li concentration profile, modified by the outdiffusion phenomenon, is strongly dependent on diffusion process parameters. A completely different behavior of Li ions in lithium niobate was obtained in samples fabricated with various methods. For example, using a 25 nm layer of MgO deposited on $LiNbO_3$ surface, a strong increase in Li outdiffusion rate was observed. Anyhow, there are various well-known methods to compensate/suppress the Li outdiffusion process.[6]

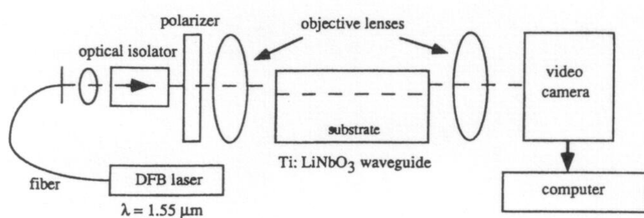

FIG. 4. Schematic diagram of the NF setup.

III. Ti:$LiNbO_3$ CHANNEL WAVEGUIDES

A. Experiment

Diffusant Ti film of 965 Å thickness was deposited by sputtering onto an X-cut $LiNbO_3$ substrate and patterned photolithographically. The strip width was 8.5 μm. Titanium was diffused at 1030 °C for 9 h under the same conditions as for the slab waveguides.

From the diffusion theory, the Ti concentration profile in a channel waveguide is given by[7]

$$C(x,z)=\frac{\tau C_0}{2\sqrt{\pi D t}}\exp\left(\frac{-x^2}{4Dt}\right)\left[\operatorname{erf}\left(\frac{z+w}{d_z}\right)-\operatorname{erf}\left(\frac{z-w}{d_z}\right)\right], \quad (5)$$

where $2w$ is the strip width, and d_z is the diffusion depth along the lateral axis. In this case, the reference coordinates have been chosen to coincide with the crystal principal axes.

NF measurements were performed with a distributed feedback (DFB) single-mode semiconductor laser diode, operating at 1.55 μm, butt-coupled to the Ti-diffused $LiNbO_3$ strip waveguide. The schematic diagram of the setup is shown in Fig. 4.

Both the launched and excited modes were transverse electric (TE) polarized. The magnified NF image of the guided mode was projected onto the infrared Hamamatsu digitizing video camera (Vidicon 1000) using a 20×, f=10 mm objective lens. A desktop computer was connected to the camera to store and manipulate the intensity data profiles which were corrected for the low-power response of the video camera, using the following equation:

$$I(x,z)=I_m(x,z)^{1/\gamma}, \quad (6)$$

where $I(x,z)$ is the calculated field power intensity, $I_m(x,z)$ is the measured intensity, and γ is the nonlinearity coefficient of the video camera. Figure 5 shows one of the measured power intensity profiles (3D plot) for the guide under investigation.

Ten intensity profiles were measured and the average profile was calculated for each guide in order to reduce the noise. The electric-field intensity was calculated using the equation

$$A(x,z)=\left(\frac{I(x,z)}{I_{\max}}\right)^{1/2}, \quad (7)$$

where $A(x,z)$ is the normalized electric field intensity and $I_{\max}$ is the maximum power intensity.

To reduce further the effects of noise, especially to eliminate the high-frequency fluctuations, the field profile

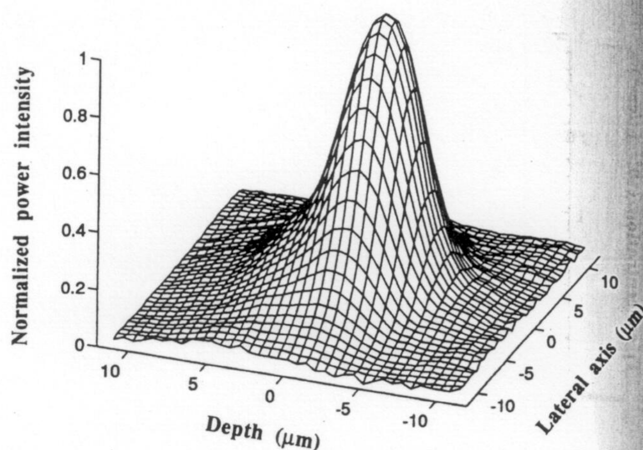

FIG. 5. Power intensity profile of the Ti:$LiNbO_3$ channel waveguide measured by NF method.

was smoothed out by a low-pass digital filter with a rejected power R=0.057%, calculated using the equation

$$R=\frac{P_i-P_0}{P_i}, \quad (8)$$

where P_i and P_0 are the input and output powers of the filter, respectively, integrated over the whole cross section S. The relative error ϵ (0.71%) between the filter input-field profile and the smoothed one was obtained from the following equation:

$$\epsilon=\frac{\int_S|A_0-A_i|ds}{\int_S A_i\, ds}, \quad (9)$$

where A_1 and A_0 are the normalized filter-input and -output electric-field intensities, respectively.

B. Results and discussions: NF analysis

It is shown that the refractive index distribution can be determined uniquely from the propagation-mode NF pattern.[15] The propagating-mode NF method has been applied to the index profile measurement for single-mode three-dimensional optical channel waveguides realized on $LiNbO_3$ by Ti indiffusion. To calculate the index profile from the smoothed electric field, it was assumed that the permeability of the medium is equal to that of vacuum and the refractive index change is very small. Maxwell's equations were approximated into the scalar wave equation,

$$\nabla^2 A(x,z)+[k^2n^2(x,z)-\beta^2]A(x,z)=0, \quad (10)$$

where $k(=2\pi/\lambda)$ is the propagation constant in free space, β $(=kN_{\text{eff}})$ is the propagation constant in the medium, N_{eff} being the effective index for the fundamental mode. Equation (10) leads to the following expression for the refractive index:

$$n^2(x,z)=\frac{\beta^2}{k^2}-\frac{1}{k^2}\frac{\nabla^2 A}{A}. \quad (11)$$

The method to construct the refractive index profile from the measured NF intensity was applied to a number of theo-

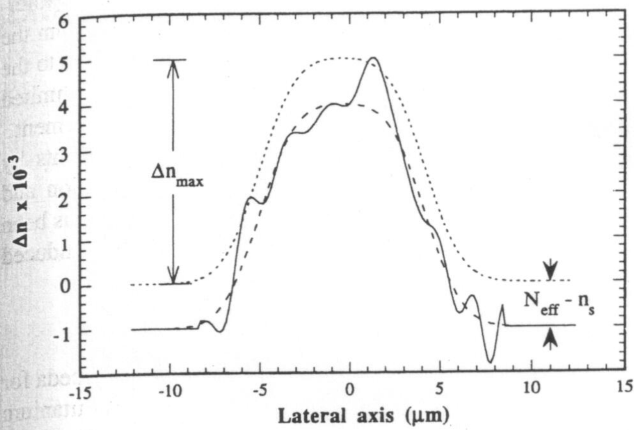

FIG. 6. Refractive index change profile obtained by NF method (solid line), best fit index profile (dashed line), and expected index profile (dotted line) for Ti:$LiNbO_3$ channel waveguide.

retical and experimental examples, as internal consistency checks. At first it was applied to some analytical examples of optical fibers and diffused waveguides, in which we found the mode profile for an imposed index profile and then, using the NF calculation procedure, the true index profile was obtained. Afterward, the method was used for various experimental examples of optical fibers, $LiNbO_3$ waveguides, and ion-exchanged glass waveguides.

In the case of Ti:$LiNbO_3$, for TE polarization and Y propagation in X-cut waveguides, electric field is along the Z axis and the refractive index is equal to the extraordinary index, which is 2.138 for $\lambda=1.55$ μm.[16] The effective index N_{eff} is very close to that of the substrate n_s and the index change Δn was measured using the NF method as follows: Let $N_{\text{eff}}=n_s$, so, using Eq. (11), the approximate expression of Δn is given by

$$\Delta n(x,z)=\left(n_s^2-\frac{1}{k^2A}\,\nabla^2 A\right)^{1/2}-n_s. \tag{12}$$

At points far from the guiding region, $\Delta n(x,z)=0$, but with

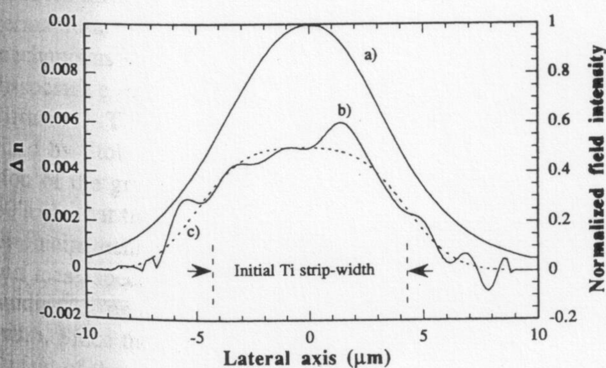

FIG. 7. Lateral cross section of: (a) measured electric-field intensity; (b) calculated refractive index profile; (c) best fit of the refractive index (b) to an error function.

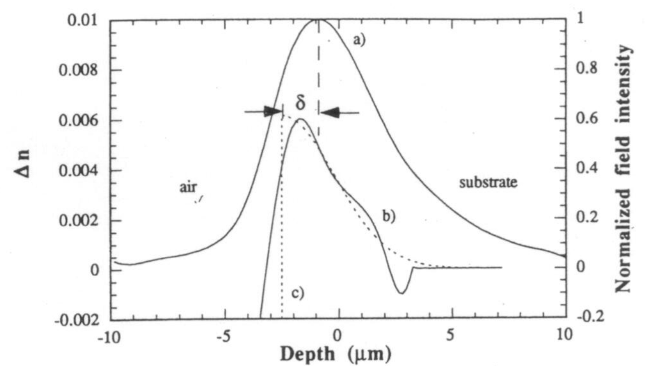

FIG. 8. Vertical section of: (a) measured electric-field intensity; (b) calculated refractive index profile; (c) best fit of the refractive index (b) to a semi-Gaussian function.

the approximation $N_{\text{eff}}=n_s$ it becomes $\Delta n(x,z)=n_s-N_{\text{eff}}$. In principle, N_{eff} can be obtained by this method, as shown in Fig. 6.

Figure 7 shows (a) horizontal sections of the measured field intensity, (b) the index profile measured by the NF method, and (c) the best fitting of the profile presented in (b) done on the basis of an error function given by

$$\Delta n(z)=\frac{\Delta n_{\max}}{2}\,\text{erf}\left(\frac{z+w}{d_z}\right)-\text{erf}\left(\frac{z-w}{d_z}\right). \tag{13}$$

Broadening of the index profile in the lateral scale with respect to the strip width is due to the lateral diffusion of Ti and can be seen in the same figure. The recovered parameters obtained from the best fitting [Eq. (13)] are $\Delta n_{\max}=0.005$, $2w=9.26$ μm, and $d_z=2.25$ μm with a relative error of about 12%.

Figure 8 presents a vertical cross section of the mode profile at the maximum value and that of the index profile fit to a semi-Gaussian function given by

$$\Delta n(x)=\Delta n_{\max}\exp(-x^2/d_x^2),\quad \text{for } x\leqslant 0. \tag{14}$$

The recovered parameters in this case are $\Delta n_{\max}=0.006$, $d_x=3.27$ μm in the depth scale with a relative error of about 20%.

The maximum of the mode profile is shifted toward the substrate by 1.56 μm (δ, as shown in Fig. 8), as in agreement with the wave theory.[17] Most of the guided mode power travels in the guide region with a small tail in the substrate, and with almost zero tail in the air side due to the high index difference between these two media.

Ideally, a Ti:$LiNbO_3$ waveguide should have a sharp steplike index difference at the air–guide interface, but as seen in Fig. 8, although there is a sharp change in the interface region, it is not an ideal step. This can be due to the diffraction phenomena at the guide end and to the limited resolution of the objective lenses in the present case (~1 μm), smoothing out the intensity mode profile before being measured by the video camera.

IV. RELATIONSHIP BETWEEN REFRACTIVE INDEX CHANGE AND DOPANT CONCENTRATION

It has been demonstrated that both refractive index and titanium concentration profiles are Gaussian. The relationship between dopant concentration C and refractive index change Δn can be derived from Eqs. (4) and (14) as follows:

$$\Delta n(C)=\Delta n_{\max}(C/C_{\max})^{\alpha}, \qquad (15)$$

where $C_{\max}$ is the maximum Ti concentration, $\alpha=(d_c/d_n)^2$, $d_c=\sqrt{4Dt}$, and d_n is the $1/e$ depth of the refractive index change profile. In our case, $\Delta n_{\max}=0.006$ and $d_n=3.27$ μm, as derived from NF measurements and $C_{\max}=7.29\times10^{20}$ atoms/cm^3 and $d_c=4.70$ μm, as derived from RBS and SIMS analyses.

Therefore, from the present studies we obtained

$$\Delta n \propto C^{2.1}. \qquad (16)$$

Equation (16) indicates a nonlinear relationship between the index change and Ti concentration inside the crystal. The proportionality constant is a function of the strip dimensions and the diffusion process parameters. Similar results were obtained by other workers[12] using different techniques to obtain dopant concentration and refractive index change profiles.

The diffusion of Ti into $LiNbO_3$ creates stresses sufficient to generate both misfit dislocations and cracks within the diffused layer.[18] The most likely mechanism for the refractive index change in the diffused layer is that due to photoelastic effect caused by the lattice contraction which increases nonlinearly with Ti concentration, explaining the behavior in Eq. (16).

V. CONCLUSIONS

The depth-diffusion behavior of Ti has been studied in Ti:$LiNbO_3$ slab waveguides by SIMS. It has been found that the main parameters that affect and control the Ti concentration depth profile are the initial thickness of the Ti film and the diffusion temperature. Anisotropy in the diffusion rate for X- and Z-cut crystal directions has been observed.

Reconstruction of the refractive index profiles in channel Ti:$LiNbO_3$ waveguides has been made by the NF method. A sharp change in the refractive index at the air–guide interface has been observed, as expected. The deviation from the ideal steplike behavior for the index change can be due to the diffraction phenomena at the guide end and by the limited resolution of the objective lenses used in the measurement.

Combining SIMS results with index measurements by NF, the relationship between the dopant concentration and index change has been found to be nonlinear, which has been attributed to a nonlinear increase in the diffusion-induced strains with dopant concentration.

ACKNOWLEDGMENTS

The authors would like to thank Professor C. Someda for his guidance and M. Elena for his help in preparing titanium films. The help of G. Caneva is also appreciated. The work of P. Chakraborty was partially supported by the International Center for Theoretical Physics, Trieste, Italy.

[1] H. Nishihara, M. Haruna, and T. Suhara, *Optical Integrated Circuits* (McGraw-Hill, New York, 1985).
[2] D. P. Birnie III, J. Mater. Sci. **28**, 302 (1993), and references therein.
[3] C. Canali, A. Carnera, G. Della Mea, P. Mazzoldi, S. M. Al Shukri, A. C. G. Nutt, and R. M. De La Rue, J. Appl. Phys. **59**, 2643 (1986).
[4] M. N. Armenise, IEE Proc. **135**, 85 (1988)
[5] P. K. Wei and W. S. Wang, IEEE Photon Technol. Lett. **PTL-6**, 245 (1994).
[6] F. Caccavale, P. Chakraborty, I. Mansour, G. Gianello, and M. Elena, J. Appl. Phys. **76**, 7552 (1994).
[7] T. Shiozawa, H. Miyamoto, H. Ohta, M. Yamaguchi, and T. Oki, IEEE J. Lightwave Technol. **LT-8**, 497 (1990).
[8] F. Gonella, F. Caccavale, and A. Quaranta, Int. J. Optoelectron. **9**, 359 (1994).
[9] A. Neyer, in Proceedings of the III European Conference ECIO'85, Berlin, Germany, 1985, p. 67.
[10] K. Morishita, IEEE J. Lightwave Technol. **LT-4**, 1120 (1986).
[11] M. Minakata, S. Saito, M. Shibata, and S. Miyazawa, J. Appl. Phys. **49**, 4667 (1978).
[12] S. Fouchet, A. Carenco, C. Daguet, R. Guglielmi, and L. Riviere, IEEE J. Lightwave Technol. **LT-5**, 700 (1987).
[13] J. Crank, *The Mathematics of Diffusion* (Clarendon, Oxford, 1975).
[14] J. R. Carruthers, I. P. Kaminow, and L. W. Stulz, Appl. Opt. **13**, 2333 (1974).
[15] L. Mc Caughan and E. E. Bergmann, IEEE J. Lightwave Technol. **LT-1**, 241 (1983).
[16] R. S. Weis and T. K. Gaylord, Appl. Phys. A **37**, 191 (1985).
[17] N. H. Zhu, X. S. Zheng, Y. K. Lin, and X. Yu, Opt. Quantum Electron. **24**, 737 (1992).
[18] K. Sugii, M. Fukuma, and H. Iwasaki, J. Mater. Sci. **13**, 523 (1978).